Adsorption 2, 299–309 (1996)

Role of Convection and Diffusion in a Single Pore with Adsorptive Walls

SYED M. TAQVI AND M. DOUGLAS LEVAN
Department of Chemical Engineering, University of Virginia, Charlottesville, VA 22903-2442, U.S.A.

Received November 14, 1995; Revised May 28, 1996; Accepted May 29, 1996

Abstract. The importance of intraparticle convection during and after the pressurization step of a pressure swing adsorption process is assessed by considering a single, cylindrical, closed-end pore with adsorptive walls exposed to a binary mixture of an adsorbable component and an inert gas. Gas-phase mass transfer is comprised of pore diffusion and convection, and surface diffusion occurs in the adsorbed phase. Concentration, velocity, and flux profiles are obtained inside the pore both during and after pressurization. Solutions are obtained analytically for the limiting cases of no adsorption, no diffusion, and no inert gas. Complete solutions of the material balance equations are obtained by orthogonal collocation. The pressurization rate, the adsorptive capacity of the pore wall, and the gas-phase mole fraction are varied over a wide range to study the relative importance of convection and diffusion under different conditions. Results show that convection makes a large contribution to transport in the pore except when the adsorbable component has a small mole fraction.

Keywords: intraparticle convection, intraparticle diffusion, pressure swing adsorption

Introduction

Mass transfer resistances inside adsorbent particles can significantly affect the performance of a pressure swing adsorption (PSA) process. This is especially true for kinetically controlled processes where the choice of cycling time is directly influenced by the rate of transport in the adsorbent particles. Also, for rapid PSA processes, the cycling time has to be very short for the process to be viable and, consequently, the mass transfer resistances have to be small.

In an adsorbent particle, mass transfer can be controlled by the macropore resistance or the micropore resistance. A semi-empirical criterion was proposed by Ruthven and Loughlin (1972) to determine the relative importance of these resistances. For the case when the macropore resistance is the controlling resistance, the overall mass transfer resistance can be reduced by using small adsorbent particles. Previous works in the literature (Sundaram and Wankat, 1988; Buzanowski et al., 1989; Rodrigues et al., 1991) have assumed the presence of small adsorbent particles and neglected mass transfer resistances completely in the analysis of rapid PSA processes. However, Lu et al. (1992a, 1992b) have shown that the use of small particles results in higher pressurization and blowdown times leading to an increase in the overall cycling time. Lu et al. (1992a) have suggested the use of large pore adsorbents in rapid PSA processes to enhance mass transfer through the particles and, thus, decrease the cycle time. In addition to the diffusional mechanisms, they have considered transport of mass by *axial* convection through the particles.

Convection can develop inside a large pore due to pressurization or blowdown. Convection can also develop as a result of adsorption and desorption. For example, more gas is drawn into the pore as a result of adsorption. Thus, convection is present inside the pores of an adsorbent particle not only during pressurization and blowdown steps of an adsorption cycle but also during the feed and purge steps. Therefore, convection can augment diffusional mass transfer in the pores as suggested by Lu et al. (1992a, 1992b).

This paper examines the relative importance of diffusion and convection in a large pore with adsorptive

walls during and after pressurization. A similar adsorptive pore model was used by Aris (1983) to evaluate the concentration dependent apparent diffusion coefficient when both gas-phase diffusion and surface diffusion are the transport mechanisms inside a pore. Our goals are to compare the relative magnitudes of diffusive and convective fluxes at different times in the pore under different conditions and thus obtain the conditions when convection plays a significant role in mass transfer through the pore.

Theory

We consider a cylindrical pore with adsorptive walls, closed at one end and exposed to the bulk fluid at the other end, as shown in Fig. 1. Under conditions of symmetry, the analysis also pertains to an open-ended pore with both ends exposed to bulk gas. The gas phase consists of adsorbable component A and inert component B.

The following assumptions are made in writing the material balance equations:

1. The gas phase is ideal.
2. There are no pressure gradients inside the pore.
3. There are no radial concentration gradients.
4. Local equilibrium is present at every cross section in the pore.
5. The adsorption isotherm for the adsorbable component is linear, i.e., $\Gamma_A = k_A c_A$.
6. Pore diffusion in the gas phase can be described by Fick's law with a constant diffusion coefficient.
7. The pore is large enough that Knudsen diffusion can be neglected (e.g., larger than 100 nm at 1 atm pressure).
8. Surface diffusion is described by a Fickian-type relation with a surface concentration gradient driving force and a constant surface diffusion coefficient.

Assumption of a constant surface diffusion coefficient is valid when the adsorption isotherm is linear (Ruthven and Kärger, 1992). We are adopting these assumptions to obtain a straightforward model with a minimum number of dimensionless groups.

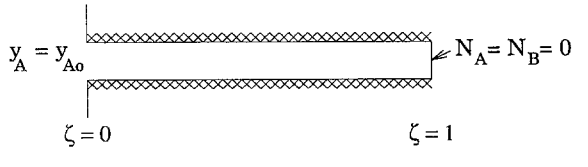

Figure 1. Closed-end cylindrical pore with adsorptive walls.

The fluxes of components A and B can be written

$$N_A = vcy_A - D_{AB}c\frac{\partial y_A}{\partial z} - D_{AS}a_v\frac{\partial \Gamma_A}{\partial z} \tag{1}$$

$$N_B = vcy_B - D_{AB}c\frac{\partial y_B}{\partial z} \tag{2}$$

The material balances within the pore are

$$a_v\frac{\partial \Gamma_A}{\partial t} + \frac{\partial c_A}{\partial t} + \frac{\partial N_A}{\partial z} = 0 \tag{3}$$

$$\frac{\partial c_B}{\partial t} + \frac{\partial N_B}{\partial z} = 0 \tag{4}$$

We define the following dimensionless variables for this problem:

$$P^* \equiv P/P_{\text{ref}}$$
$$\zeta \equiv z/L$$
$$\tau \equiv D_{AB}t/L^2$$
$$v^* \equiv vL/D_{AB}$$
$$\Gamma_A^* \equiv \Gamma_A RT/k_A P_{\text{ref}}$$

The dimensionless flux of component A can be written

$$N_A^* \equiv \frac{N_A}{N_{A_{\text{ref}}}} = P^*\left[v^* y_A - \frac{\partial y_A}{\partial \zeta} - (k_A a_v)\left(\frac{D_{AS}}{D_{AB}}\right)\frac{\partial y_A}{\partial \zeta}\right] \tag{5}$$

where

$$N_{A_{\text{ref}}} \equiv \frac{P_{\text{ref}}D_{AB}}{RTL} \tag{6}$$

The material balance equations become

$$(k_A a_v + 1)\frac{\partial y_A}{\partial \tau} + \frac{\partial v^* y_A}{\partial \zeta} - \left(1 + k_A a_v \frac{D_{AS}}{D_{AB}}\right)\frac{\partial^2 y_A}{\partial \zeta^2} = -(k_A a_v + 1)y_A\frac{1}{P^*}\frac{dP^*}{d\tau} \tag{7}$$

$$\frac{\partial y_B}{\partial \tau} + \frac{\partial v^* y_B}{\partial \zeta} - \frac{\partial^2 y_B}{\partial \zeta^2} = -y_B\frac{1}{P^*}\frac{dP^*}{d\tau} \tag{8}$$

where $k_A a_v$ is the dimensionless partition ratio representing the adsorptive capacity of the pore wall relative to the fluid-phase concentration. Writing Eq. (8) in terms of y_A and eliminating $\partial y_A/\partial \tau$ between the resulting equation and Eq. (7) gives

$$-k_A a_v \frac{\partial y_A}{\partial \zeta} v^* + [k_A a_v (1 - y_A) + 1] \frac{\partial v^*}{\partial \zeta} = -(k_A a_v + 1) \frac{1}{P^*} \frac{dP^*}{d\tau} - k_A a_v \left(1 - \frac{D_{AS}}{D_{AB}}\right) \frac{\partial^2 y_A}{\partial \zeta^2} \tag{9}$$

For boundary conditions, at the closed end of the pore the flux is zero and at the open end of the pore we will assume that a constant mole fraction exists at all times. The boundary conditions at the closed end of the pore are

$$\frac{\partial y_A}{\partial \zeta} = 0 \quad \text{and} \quad v^* = 0 \quad \text{at } \zeta = 1 \tag{10}$$

while at the open end of the pore we have

$$y_A = y_{Ao} \quad \text{at } \zeta = 0 \tag{11}$$

where y_{Ao} is a constant. The velocity at the open end of the pore can be obtained by integrating Eq. (9) over the entire length of the pore to obtain

$$[k_A a_v (1 - y_{Ao}) + 1] v^*|_{\zeta=0} = (k_A a_v + 1) \frac{1}{P^*} \frac{dP^*}{d\tau} - k_A a_v \left(1 - \frac{D_{AS}}{D_{AB}}\right) \left.\frac{\partial y_A}{\partial \zeta}\right|_{\zeta=0} \tag{12}$$

The pore wall is assumed to be in equilibrium with the gas phase prior to pressurization. Therefore, the initial conditions are

$$y_A = y_{Ao} \quad \text{and} \quad v^* = 0 \quad \text{at } \tau = 0 \tag{13}$$

Equations (7) and (9) can be solved with Eqs. (10)–(13) to obtain the concentration and velocity profiles inside the pore at any time.

The first term on the right hand side of Eq. (5) is the convective flux, the second term represents pore diffusion in the gas phase, and the third term describes surface diffusion in the adsorbed phase. As a result of pressurization and concentration gradients developed during pressurization, these transport mechanisms transfer material to the closed end of the pore. The relative magnitudes of the contributions to flux in Eq. (5) depend at any time on the rate of pressurization, the mole fraction of A in the gas phase, the adsorptive capacity of the pore wall, and the ratio of the surface diffusion coefficient to the pore diffusion coefficient. We will vary several of these parameters to study the relative contribution of convection and pore diffusion to gas-phase mass transport. The effect of surface diffusion on gas-phase mass transfer is also studied whenever surface diffusion makes a significant contribution to the total flux in the pore.

Limiting Cases

Under certain limiting conditions it is possible to obtain the solutions to the material balance equations analytically.

No Adsorption

For the limiting case of no adsorption, the mole fraction inside the pore remains the same at all times, and the velocity inside the pore can be obtained by integration of Eq. (8) to give

$$v^* = \frac{1}{P^*} \frac{dP^*}{d\tau} (1 - \zeta) \tag{14}$$

For this case, convection occurs only during pressurization and the velocity is directly proportional to the rate of pressurization and inversely proportional to the total pressure. This solution will be useful in showing the increase in convection due to the existence of adsorption.

No Diffusion

Another limiting case is pressurization in the absence of diffusion. This case is approached asymptotically when the diffusion time is very large compared to the pressurization time or when the adsorptive capacity of the pore wall is very large. Mathematically, the problem resembles the pressurization of an adsorption bed with local equilibrium as considered by Knaebel and Hill (1984), and the solutions obtained are similar.

The dimensionless equations obtained above cannot be used for this case as the diffusion time and diffusion velocity are not defined. However, nondimensionalization can still be carried out by defining a reference velocity as

$$v_{\text{ref}} \equiv L\frac{dP^*}{dt} \tag{15}$$

and eliminating dP^*/dt from the material balance equations, Eqs. (3) and (4), to obtain

$$(k_A a_v + 1)P^*\frac{\partial y_A}{\partial P^*} + P^*\frac{\partial v^* y_A}{\partial \zeta} + y_A(k_A a_v + 1) = 0 \tag{16}$$

and

$$P^*\frac{\partial y_B}{\partial P^*} + P^*\frac{\partial v^* y_B}{\partial \zeta} + y_B = 0 \tag{17}$$

By eliminating $\partial y_A/\partial P^*$ from Eqs. (16) and (17) and integrating the resulting equation, the dimensionless velocity at any position in the pore is obtained as

$$v^* = \frac{(k_A a_v + 1)(1-\zeta)}{P^*[k_A a_v(1-y_A)+1]} \tag{18}$$

The dependence of the velocity on the feed concentration and on the adsorptive capacity of the walls of the pore becomes apparent from this expression. Since $0 \leq (1 - y_A) \leq 1$, velocity will generally increase with an increase in adsorptive capacity or feed concentration.

Following Knaebel and Hill, Eqs. (16) and (17) can be combined to obtain

$$[k_A a_v(1-y_A)+1]\frac{\partial y_A}{\partial P^*} + v^*\frac{\partial y_A}{\partial \zeta} = -\frac{1}{P^*}k_A a_v(1-y_A)y_A \tag{19}$$

The characteristic equations for this partial differential equation are

$$\frac{\partial \zeta}{\partial s} = v^* \tag{20}$$

$$\frac{\partial P^*}{\partial s} = k_A a_v(1-y_A)+1 \tag{21}$$

and

$$\frac{\partial y_A}{\partial s} = -\frac{1}{P^*}\frac{k_A a_v(1-y_A)y_A}{k_A a_v(1-y_A)+1} \tag{22}$$

where s is the characteristic direction. Combining Eqs. (21) and (22) we get the variation of the mole fraction due to a pressure shift in the characteristic direction as

$$\frac{y_A}{y_{Ao}} = \left(\frac{1-y_A}{1-y_{Ao}}\right)^{\frac{1}{k_A a_v+1}}\left(\frac{P^*}{P_o^*}\right)^{-\frac{-k_A a_v}{k_A a_v+1}} \tag{23}$$

Similarly, Eqs. (20) and (22) can be combined to obtain

$$\frac{1-\zeta}{1-\zeta_o} = \left(\frac{y_A}{y_{Ao}}\right)^{\frac{1}{k_A a_v}}\left(\frac{1-y_A}{1-y_{Ao}}\right)^{-\frac{k_A a_v+1}{k_A a_v}} \times \left(\frac{1+k_A a_v(1-y_A)}{1+k_A a_v(1-y_{Ao})}\right) \tag{24}$$

where the subscript o denotes the initial condition. The mole fraction profiles obtained from using Eqs. (23) and (24) for a change of pressure from 1 to 10 atmospheres are shown in Fig. 2. A value of 10 was used for the adsorptive capacity of the pore wall ($k_A a_v$). Solutions were obtained at different bulk gas-phase mole fractions of component A. The part of the profile where the mole fraction is constant corresponds to characteristics present in the pore before the start of pressurization. Convection develops as a result of pressurization and transports material towards the closed end of the pore. Mathematically, this corresponds to the entrance of new characteristics into the pore. The magnitude of the convective flux increases with an increase in the mole fraction of component A as evident from the large penetration into the pore of the new characteristics at $y_{Ao} = 0.99$ (Fig. 2(c)).

Pure Adsorbable Component

Another limiting case that can be considered is when the feed consists of only the adsorbable component A. For this case the material balance equation for component A can be integrated to obtain the velocity profile inside the pore as

$$v^* = (k_A a_v + 1)(1-\zeta)\frac{1}{P^*}\frac{dP^*}{d\tau} \tag{25}$$

Thus, convection is directly proportional to the rate of pressurization and becomes nonexistent after pressurization is complete.

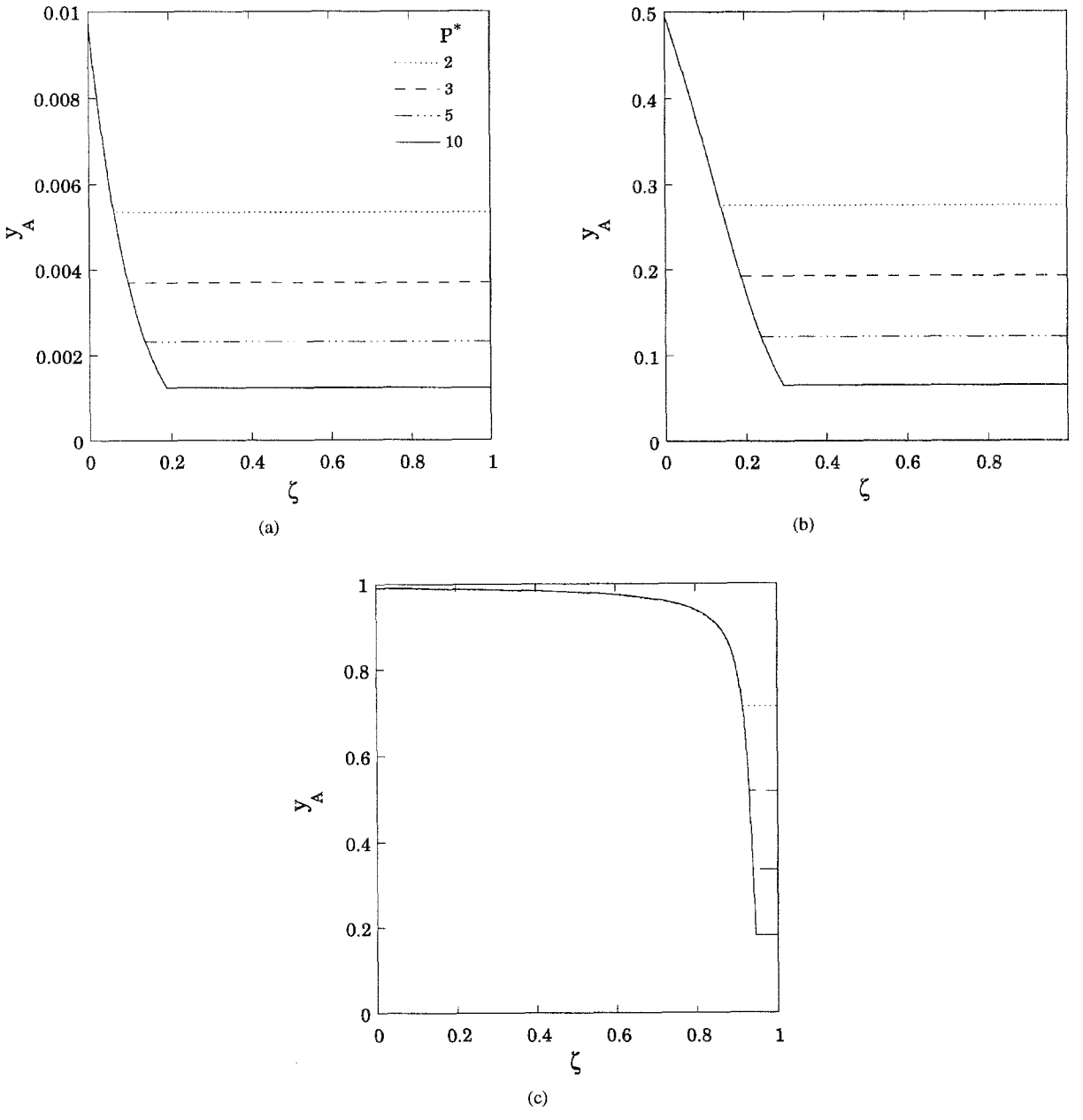

Figure 2. Pressurization of a closed-end pore in the absence of diffusion with $k_A a_v = 10$: (a) $y_{Ao} = 0.01$; (b) $y_{Ao} = 0.5$; (c) $y_{Ao} = 0.99$. Legend for (b) and (c) is the same as for (a). Note change in scale of y-axis.

Numerical Solution

The complete solution of the pair of partial differential equations, Eqs. (7) and (9), was obtained by orthogonal collocation. Legendre polynomials were used to obtain collocation points inside the pore. We used 16 internal collocation points. At each collocation point, Eq. (7) reduces to an ordinary differential equation in time and Eq. (9) reduces to an algebraic equation. The set of equations was solved to obtain v^* and $\partial y_A/\partial\tau$ at each collocation point and $\partial y_A/\partial\tau$ was integrated using the Gear's method solver LSODE (Hindmarsh, 1980) to obtain the mole fraction profile inside the pore.

We assume that the pore is initially in equilibrium with the gas phase at one atmosphere. The pore is then pressurized to 5 atmospheres over a short time interval. The mole fraction of component A in the bulk gas at the pore mouth remains constant at all times. Diffusion coefficients were chosen to be 10^{-5} m^2/s for D_{AB} and 10^{-7} m^2/s for D_{AS} (Ruthven and Kärger, 1992). Parameters varied were the mole fraction of A at the pore mouth (y_{Ao}), the pressurization rate ($dP^*/d\tau$), and the adsorptive capacity ($k_A a_v$).

We assumed a pore length of 0.01 cm to 0.1 cm. It is interesting to calculate approximate values for gas-phase diffusion times for this problem and compare them to the pressurization time. For a PSA process, the pressurization step is often about 1 to 4 seconds long. For a pore of length 0.01 cm, the diffusion time (L^2/D_{AB}) is 0.001 seconds. For a larger pore with $L = 0.1$ cm, the diffusion time is 0.1 seconds. Thus, the diffusion time is small compared to the pressurization time, and diffusion can contribute significantly to the overall transport even during rapid pressurization. The effect of adsorption capacity on this comparison is considered below.

Considering pressurization times, for a rapid pressurization with a pressurization time of 1 second, the dimensionless pressurization rate, $dP^*/d\tau$, for a change of total pressure from one atmosphere to 5 atmospheres is 0.004 for the 0.01 cm pore and 0.4 for the 0.1 cm pore. For a pressurization time of 4 seconds, the dimensionless pressurization rate is 0.001 for the smaller pore and 0.1 for the larger pore. Thus, the dimensionless pressurization rate can vary from roughly 0.001 to 0.4.

Base Case

The first case that we have considered is $dP^*/d\tau = 0.001$, $k_A a_v = 10$, and $y_{Ao} = 0.5$. The velocity profiles are shown in Fig. 3(a). Pressurization is complete at $\tau = 4000$. For comparison, the velocity profiles obtained in the absence of adsorption, obtained from Eq. (14) are also shown by dashed lines. Convection is present only during pressurization in the absence of adsorption. On the other hand, when the pore wall is adsorptive, there is a large increase in the velocity during pressurization and convection is present even after pressurization is complete. We mentioned earlier that convection occurs as a result of pressurization and can also be induced by adsorption. This figure clearly shows the importance of adsorption induced convection. For the same pressurization rate, there is a large increase in the convective flux when the pore wall is adsorptive.

The corresponding mole fraction profiles are shown in Fig. 3(b). Initially, the mole fraction in the gas phase decreases due to adsorption on the walls of the pore. However, both convection and diffusion transport material towards the pore end and the mole fraction gradually goes back to the initial equilibrium value. Since pressurization is slow, the system reaches close to the equilibrium value during pressurization.

The convective and diffusive fluxes for component A in the gas phase are shown in Figs. 3(c) and (d). Convection and diffusion contribute roughly equally to transport in the pore both during and after pressurization. For this case, $(k_A a_v)(D_{AS}/D_{AB}) = 0.1$ and the contribution of surface diffusion is small compared to the contributions of the different gas-phase fluxes.

Fast Pressurization

The effects of increasing the pressurization rate to 0.4 are shown in Fig. 4. Rapid pressurization results in large velocities and large mole fraction gradients in the gas phase. Hence, both convective and diffusive fluxes increase but remain of equal magnitudes.

Large Partition Ratio

There is an increase in both convection and diffusion on increasing the adsorptive capacity of the pore walls. In addition, the time taken to reach equilibrium increases. Figures 5(a) and (b) show the convection and diffusion fluxes when the dimensionless parameter $k_A a_v$ has been increased to 1000. For this case, $(k_A a_v)(D_{AS}/D_{AB}) = 10$ and, therefore, surface diffusion is a significant mechanism of transport inside the pore. The influence of surface diffusion can be shown by plotting the convective and pore diffusive fluxes in the absence of surface diffusion, i.e., with $D_{AS} = 0$. In the absence of surface diffusion, the driving force for both convection and diffusion increases, and an increase (by a factor of about 5) in both fluxes is observed as shown in Figs. 5(c) and (d). In addition, there is a large increase in the time taken to reach equilibrium.

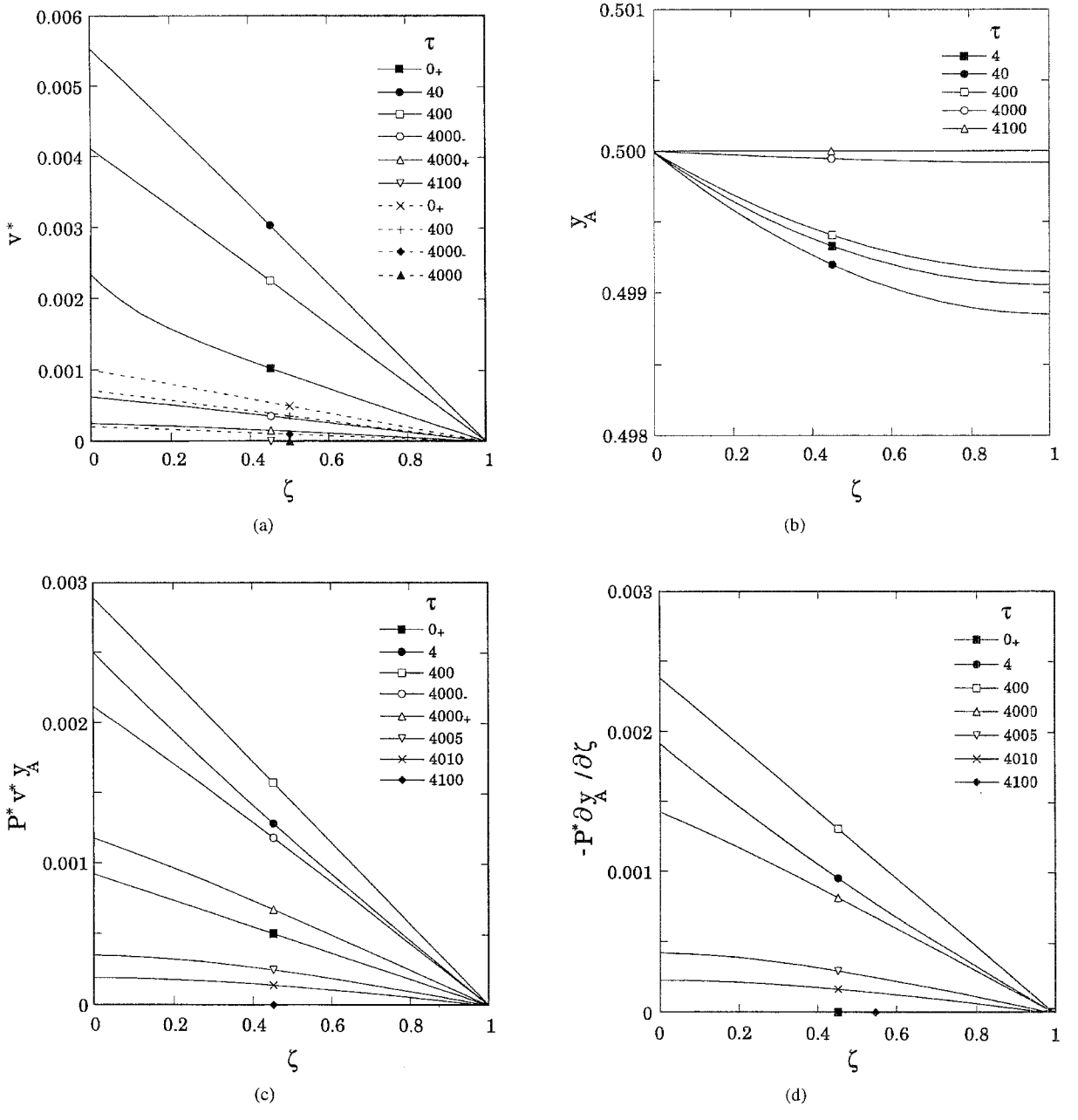

Figure 3. Pressurization of a closed-end pore with $dP^*/d\tau = 0.001$, $k_A a_v = 10$, $\tau' = 4000$, and $y_{Ao} = 0.5$: (a) Velocity profiles with dashed lines denoting absence of adsorption; (b) Mole fraction profiles; (c) Convective flux profiles; (d) Gas-phase diffusive flux profiles.

Bulk Gas-Phase Mole Fraction Variation

In the absence of surface diffusion, the flux of component A can be written

$$N_A = -D_{AB}c\frac{\partial y_A}{\partial z} + y_A(N_A + N_B) \qquad (26)$$

where the first term on the right hand side is the diffusive flux of A and the second term is the convective flux. From this equation we can easily obtain

$$\frac{\text{Convective flux of } A}{\text{Diffusive flux of } A} = \frac{y_A(N_A + N_B)}{(1 - y_A)N_A - y_A N_B} \qquad (27)$$

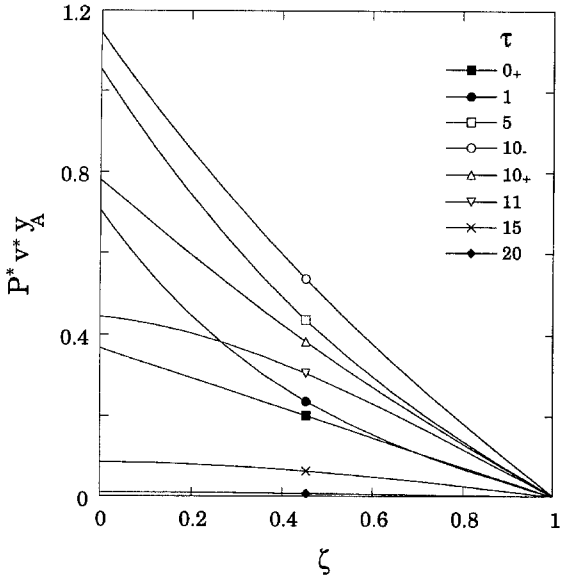

Figure 4. Pressurization of a closed-end pore with $dP^*/d\tau = 0.4$, $k_A a_v = 10$, $\tau' = 10$, and $y_{Ao} = 0.5$: (a) Convective flux profiles; (b) Gas-phase diffusive flux profiles.

In Fig. 6 the ratio of convective flux to diffusive flux is shown as a function of y_A for different values of N_B. Two convenient limits, but not real limits for this process, are equimolar counterdiffusion and diffusion through a stagnant gas. In the limit of equimolar counterdiffusion, $N_A + N_B = 0$, and the ratio is zero for any mole fraction. For the other limiting case of diffusion through a stagnant gas, $N_B = 0$, and the ratio of convective flux to diffusive flux is $y_A/(1 - y_A)$. It is apparent from this figure that when $|N_B| \ll |N_A|$, the convective flux of A is much greater than the diffusive flux as its mole fraction approaches unity. In the limit when the gas phase consists of pure A, the diffusive flux becomes zero. On the other hand when the mole fraction is very small, diffusion is the dominating mass transfer mechanism in the gas phase.

The dependence of convection and pore diffusion on the rate of pressurization and adsorptive capacity are similar. Therefore, we have varied these parameters over a wide range and considered different combinations to study the relative importance of convection and diffusion at very high and very low gas phase mole fraction of the adsorbable component. Whenever surface diffusion is significant ($k_A a_v D_{AS}/D_{AB} \geq O(1)$), we have also examined the effect of the absence of surface diffusion. The results are shown in Table 1 for $y_A = 0.01$ and in Table 2 for $y_A = 0.99$.

$y_{Ao} = 0.01$. In Table 1 we have listed the ratio of the convective flux to the diffusive flux just before and

Table 1. Ratio of convective flux to diffusive flux of component A at the pore opening and near the closed end of the pore before and after the end of pressurization for $y_{Ao} = 0.01$.

			$(v^* y_A)/(-\partial y_A/\partial\zeta)$			
			$\tau = \tau'_-$		$\tau = \tau'_+$	
$dP^*/d\tau$	$k_A a_v$	D_{AS}	$\zeta = 0$	$\zeta \to 1$	$\zeta = 0$	$\zeta \to 1$
0.001	10	10^{-7}	0.279	0.232	0.0091	0.0091
0.4	10	10^{-7}	0.143	0.087	0.0091	0.0061
0.4	1000	10^{-7}	0.041	0.038	0.0100	0.0022
0.4	1000	0	0.022	–	0.0101	–
0.001	1000	10^{-7}	0.025	0.022	0.0100	0.0099
0.001	1000	0	0.011	0.010	0.0100	0.0091

Table 2. Ratio of convective flux to diffusive flux of component A at the pore opening and near the closed end of the pore before and after the end of pressurization for $y_{Ao} = 0.99$.

			$(v^* y_A)/(-\partial y_A/\partial\zeta)$			
			$\tau = \tau'_-$		$\tau = \tau'_+$	
$dP^*/d\tau$	$k_A a_v$	D_{AS}	$\zeta = 0$	$\zeta \to 1$	$\zeta = 0$	$\zeta \to 1$
0.001	10	10^{-7}	113.6	113.4	8.91	8.91
0.4	10	10^{-7}	109.8	69.97	8.91	8.48
0.4	1000	10^{-7}	112.3	0.311	89.10	0.28
0.4	1000	0	124.8	–	90.00	–
0.001	1000	10^{-7}	101.3	91.77	89.10	82.84
0.001	1000	0	101.8	91.16	89.99	83.20

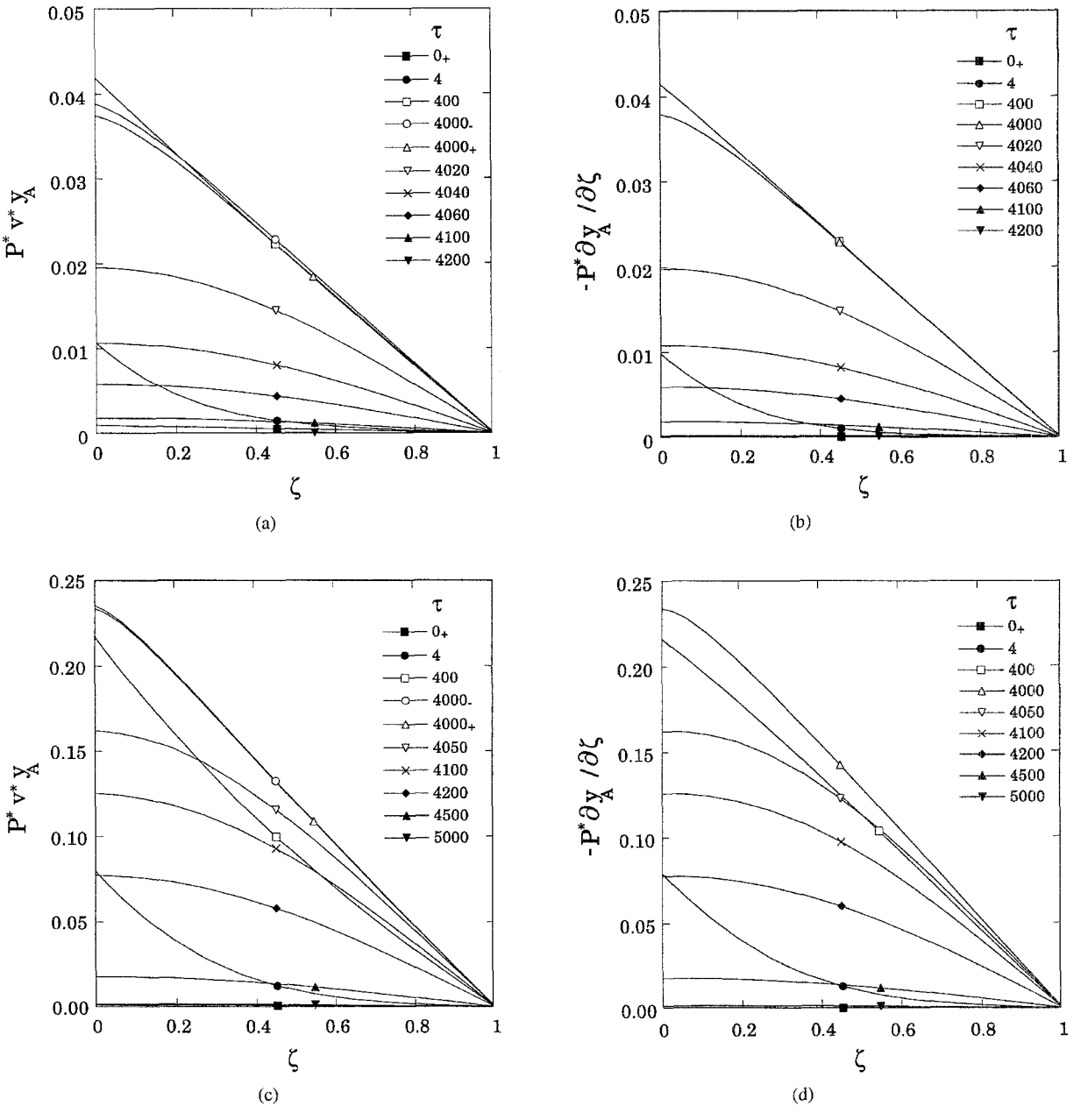

Figure 5. Pressurization of a closed-end pore with $dP^*/d\tau = 0.001$, $k_A a_v = 1000$, $\tau' = 4000$, and $y_{Ao} = 0.5$: (a) Convective flux profiles; (b) Gas-phase diffusive flux profiles; (c) Convective flux profiles, $D_{AS} = 0$; (d) Gas-phase diffusive flux profiles, $D_{AS} = 0$. Note change in scale of y-axis.

after the end of pressurization, both at the pore opening and near the closed end of the pore. Several conclusions can be drawn from this table. For all conditions, the convective flux is negligible compared to the diffusive flux after pressurization. During pressurization, the convective flux is about 8 to 30% of the diffusive flux when the adsorptive capacity of the pore walls is low. However, when the adsorptive capacity is large, the convective flux is less than 5% of the diffusive flux even during pressurization. Absence of surface diffusion makes the ratio of convective flux to diffusive flux smaller. During rapid pressurization, absence of surface diffusion results in very small values of the fluxes near the closed end of the pore.

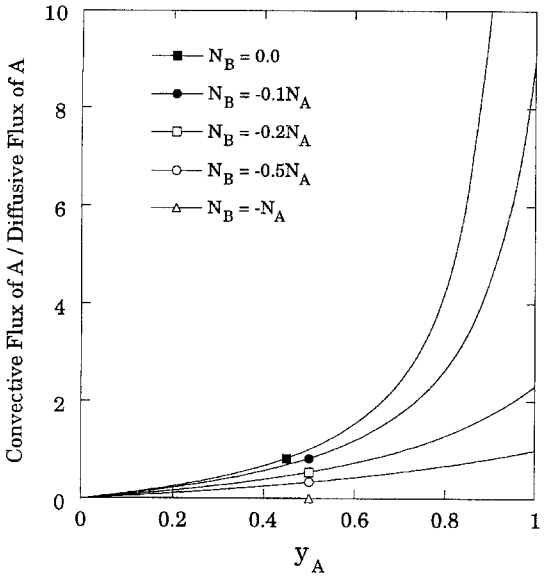

Figure 6. Ratio of convective flux of A to the diffusive flux of A as a function of y_A in the absence of surface diffusion.

$y_{Ao} = 0.99$. Table 2 shows the ratio of the convective flux to the diffusive flux just before and after the end of pressurization at the pore opening and near the closed end of the pore for $y_{Ao} = 0.99$. Diffusion is negligible both during and after pressurization when the pressurization rate is low and the adsorptive capacity of the pore walls is large. For a low adsorptive capacity and any pressurization rate, the diffusive flux is less than 2% of the convective flux during pressurization. However, for this case, diffusion can make a significant contribution to the flow after pressurization and can be greater than 10% of the convective flux. For the case when pressurization is rapid and the adsorptive capacity is very high, diffusion is negligible at the pore opening but can be more than 3 times the convective flux near the closed end of the pore. For this case also, absence of surface diffusion under these conditions results in very small values of the fluxes near the closed end of the pore.

Discussion

Various operating conditions were considered in the previous section by varying dimensionless parameters to show the relative importance of convection compared to gas-phase diffusion for transport of material in the pore. Several additional observations pertaining to mass transfer in the pore can be made from these results.

Diffusion always evolves slowly compared to convection because gradients for diffusion are developed by convection. This is most apparent from the convective and diffusive flux profiles for a low value of the adsorption capacity (Figs. 3 and 4).

There is a sudden decrease in the velocity and, hence, in the convective flux at the end of pressurization for all cases that were considered except when the pressurization is very slow and the adsorption capacity is very large (Fig. 5). For this case, convection is primarily adsorption induced and has a weak dependence on the rate of pressurization. Diffusion always develops and ends slowly and the diffusive flux does not exhibit a sharp decrease at the end of pressurization.

Under certain conditions, the relative contributions of convection and pore diffusion to transport inside the pore can change drastically along the length of the pore. In Table 2, diffusion is negligible at the pore opening during and after pressurization when the pressurization rate and adsorption capacity are very large. However, near the closed end of the pore, the diffusive flux is 3 times the convective flux.

Surface diffusion can influence gas-phase transport in different ways depending on the magnitude of the gas-phase diffusive flux and the dimensionless parameters $k_A a_v$ and D_{AS}/D_{AB}. When $y_{Ao} = 0.5$ and $k_A a_v$ is very large, the absence of surface diffusion leads to a large increase in the convective and gas-phase diffusive fluxes. However, the effect of surface diffusion can be negligible even at a high adsorption capacity when convection is the dominant mechanism for gas-phase transport.

Conclusions

The importance of intraparticle convection during and after pressurization of a PSA process has been studied by considering a binary mixture of an adsorbable component and an inert component and a single, large pore with adsorptive walls. Analytical solutions were obtained for several limiting cases. The complete solution to the material balance equations was obtained numerically.

At very low mole fraction of the adsorbable component, convection is negligible compared to diffusion after pressurization is complete. During pressurization, the convective flux inside the pore contributes significantly to the overall transport rate when the adsorptive capacity of the pore wall is small. For all other conditions at a low mole fraction of the

adsorbable component, convection can be neglected during pressurization.

When the adsorbable component is not a trace component, convection is as important as diffusion and should not be neglected in accurately describing the flux in the pore.

In the limiting case when the mole fraction of the adsorbable component approaches unity, convection becomes the dominant mass transfer mechanism. This limit is approached quickly unless the pressurization rate and the adsorptive capacity are very large, in which case the diffusive flux can be quite large near the closed end of the pore in comparison to the convective flux.

Nomenclature

a_v: surface area of the pore wall per unit volume, m^2/m^3
c: gas-phase concentration, mol/m^3
D_{AB}: gas-phase diffusion coefficient, m^2/s
D_{AS}: surface diffusion coefficient of component A, m^2/s
k_A: linear isotherm constant for component A, m
L: length of the pore, m
N: flux, mol/m^2s
P: pressure, N/m^2
R: gas constant, Pa m^3/mol K
s: characteristic direction
t: time, s
T: temperature, K
v: molar average velocity, m/s
y: gas-phase mole fraction
z: axial coordinate, m

Greek Letters

Γ: surface concentration, mol/m^2
ζ: dimensionless axial coordinate
τ: dimensionless time
τ': dimensionless pressurization time

Subscripts

A, B: component
o: initial condition
ref: reference quantity

References

Aris, R., "Interpretation of Sorption and Diffusion Data in Porous Solids," *Ind. Chem. Engng Fundam.*, **22**, 150–151 (1983).

Buzanowski, W.A., R.T. Yang, and O.W. Hass, "Direct Observation of the Effects of Bed Pressure Drop on Adsorption and Desorption Dynamics," *Chem. Engng. Sci.*, **44**, 2392–2394 (1989).

Hindmarsh, A.C., "LSODE and LSODI, Two New Initial-Value Ordinary Differential Equation Solvers," *ACM-SIGNUM Newsletter*, **15**(4), 10–11 (1980).

Knaebel, K.S. and F.B. Hill, "Pressure Swing Adsorption: Development of an Equilibrium Theory for Gas Separations," *Chem. Engng. Sci.*, **40**, 2351–2360 (1984).

Lu, Z., J.M. Loureiro, M.D. LeVan, and A.E. Rodrigues, "Intraparticle Convection Effect on Pressurization and Blowdown of Adsorbers," *AIChE J.*, **38**, 857–867 (1992a).

Lu, Z., J.M. Loureiro, M.D. LeVan, and A.E. Rodrigues, "Effect of Intraparticle Forced Convection on Gas Desorption from Fixed Beds Containing "Large-Pore" Adsorbents," *Ind. Engng. Chem. Res.*, **31**, 1530–1540 (1992b).

Rodrigues, A.E., J.M. Loureiro, and M.D. LeVan, "Simulated Pressurization of Adsorption Beds," *Gas Sep. and Purif.*, **5**, 115–124 (1991).

Ruthven, D.M. and K.F. Loughlin, "The Diffusional Resistance of Molecular Sieve Pellets," *Can. J. Chem. Engng.*, **50**, 550–552 (1972).

Ruthven, D.M. and J. Kärger, *Diffusion in Zeolites and Other Microporous Solids*, Chaps. 1 and 11. Wiley Interscience, New York, (1992).

Sundaram, N. and P.C. Wankat, "Pressure Drop Effects in the Pressurization and Blowdown Steps of Pressure Swing Adsorption," *Chem. Engng. Sci.*, **43**, 123–129 (1988).